JOURNAL OF MATERIALS SCIENCE **36** (2001) 4927–4941

A stochastic lifing method for materials operating under long service conditions: with application to the creep life of a commercial titanium alloy

M. EVANS
Department of Materials Engineering, University of Wales Swansea, Singleton Park, Swansea, UK, SA2 8PP
E-mail: m.evans@swansea.ac.uk

This paper extends the theta prediction methodology so that life predictions for materials operating under long service conditions can be made that also have a degree of confidence associated with them. Ways in which this model can be applied to the fatigue as well as the creep of all materials is also discussed. For comparison purposes two failure criteria are built into the stochastic model and the determinants of failure derived. This stochastic theta model is then used to investigate the nature of the creep failure time distribution for the Ti 6.2.4.6 alloy under constant uniaxial conditions. The distributions for each θ_j were found to be very different—with only some of them being normally distributed. The others had very pronounced skews to both the left and right. The empirical distributions for predicted failure times were also found to have long tails reaching out to higher failure times—although the failure time distributions were more symmetric when using the Monkman—Grant failure criteria. For Titanium 6.2.4.6 operating at 773 K and 580 MPa the chances of failure before 410 hours is 1%. At 480 MPa and 773 K the chances of failure before 780 hours is 1%.

1. Introduction

Today there are a wide range of materials available for a designer to choose from and a correspondingly wide range of properties. Thus medium density polyethylene plastics are now commonly used in distribution lines for water and gas, whilst reinforced resins (such as carbon fibre epoxy) are used at the cold (fan) end of modern aero engines. Titanium alloys and engineering ceramics are now extensively used at the high temperature end of aero engines, whilst low alloy steels are commonly used for the boiler tubes and pressure vessels associated with energy conversion.

In many of these applications these materials are expected to reliably perform a particular function, (i.e. with low probability of failure), and over quite long periods of time. Unexpected failures can turn out to be catastrophic and very expensive and so there is a great need to be able to extrapolate to longer term service conditions from short term tests. In this way unplanned failures can be avoided. Ideally, any such lifing method should be able to produce a life prediction together with an estimate of the confidence in that prediction.

Often the mechanisms of failure, such as slow crack growth in ceramics, stress corrosion in metals, fatigue crack growth, creep rupture in metals and pressurised plastics, can be seen to have a deceleration then a steady state and a final acceleration when plotted on appropriate axis. The theta extrapolation model is a general technique that can be applied whenever this pattern of damage accumulation exists. The technique has been extensively applied to the creep of various metals [1–3] and has proved to be a very effective method for predicting creep life. However, its application to the fatigue of metals and the creep of plastics and other materials has been very limited.

The objectives of this paper are therefore three fold. Currently, the theta model produces either a single life time prediction (for a particular set of operating conditions) or a partial analysis of the confidence associated with such a prediction. This confidence interval does not take into account all the sources of uncertainty associated with the prediction and it is also based on the arbitrary assumption of a normal distribution. The main objective of this paper is therefore to modify the theta model so as to make it fully stochastic. All the determinants of a life time prediction are given a generalised gamma distribution (for which the normal distribution is a special case) and these are then bought together using a Monte Carlo simulation to produce a distribution for the life time prediction associated with a particular operating condition.

The second objective of this paper is to apply this new stochastic theta model to the creep behaviour of the Ti 6.2.4.6 alloy. Unlike Ti-4Sn-4A1-4Mo-0.5Si (IMI 551) [4], which must operate at temperatures below 723 K, both IMI 834 and Ti 6.2.4.6 [5] are capable of operating in the 773 K to 900 K temperature range. As a result these alloys are now being used in the manufacture of

intermediate to high power (as opposed to the traditional low power role of titanium) compressor disks and blades for modern aero engines. However, at these higher operating temperatures, conditions are ideal for creep at significant rates and so it is very important to have some understanding of the creep behaviour of the Ti 6.2.4.6 alloy. As a first step in this direction this paper concentrates on the uniaxial creep behaviour of this alloy—with the intention of publishing multiaxial behaviour in a future paper.

Thirdly, it is hoped that readers of this paper will be encouraged to apply this technique to the creep of other materials (particularly plastics) and also to the fatigue of various materials. Ways in which the theta model can be applied to fatigue data are therefore briefly discussed.

To achieve these aims the first section of this paper will formulate the stochastic theta projection model within the context of creep life prediction. In this section the theta model is made stochastic by identifying, through the application of some standard statistical techniques, distributions for the determinants of time to failure (for example the theta distributions). Monte Carlo analysis is then used to combine these determinants of failure into an empirical failure time distribution. A short section then follows which suggests ways in which this technique could be applied to fatigue data. The next two sections then illustrate the way in which this model can be used to predict the uniaxial creep life of the Ti 6.2.4.6 alloy. Thus the test material and the test matrix used are described and empirical distributions for a failure time prediction at two illustrative test conditions are identified. The major determinants of the failure time distribution will also be identified in this section. In a final section conclusions and suggestions for future research are given.

2. A stochastic θ projection model

The stochastic θ projection technique has four basic steps. First, there is the experimental stage where uniaxial constant stress creep curves are measured over a range of stresses and sometimes temperatures and each creep curve is given a mathematical form. Second, the form of these creep curves is projected to other stresses and temperatures— either within (i.e. interpolation) or outside (i.e. extrapolation) the original range of test conditions. Thirdly, predictions for mean creep properties (such as the average minimum creep rate or average time to failure) are derived numerically from the projected creep curves. Finally, Monte Carlo analysis is used to obtain an empirical distribution for a predicted creep property, i.e. a creep property prediction together with a confidence in such a prediction. This rest of this section is organised into these stages.

2.1. A mathematical form for a measured creep curve

A single creep curve at steady uniaxial stress τ and absolute temperature T can be modelled using a general functional form

$$\varepsilon_t = \eta(t, \theta_1, \theta_2, \ldots, \theta_j, \ldots, \theta_m), \qquad (1a)$$

where η is some non-linear function, ε_t is the uniaxial creep strain at time t and θ_j are numerical parameters that can be determined from the experimental creep curves using a suitable estimation technique.

A variety of different equations have been used in the past to describe the form of η in Equation 1a [6, 7]. A more recent and very popular form that has also been shown to give a good representation (at least for large strains) of an experimental creep curve [8] is

$$\varepsilon_t = \theta_1(1 - e^{-\theta_2 t}) + \theta_3(e^{\theta_4 t} - 1) + \nu_t, \qquad (1b)$$

or even more recently [9],

$$\varepsilon_t = \theta_1(1 - e^{-\theta_2 t}) + \theta_3(e^{\theta_4 t} - 1) + \theta_5(1 - e^{-\theta_6 t}) + \nu_t. \qquad (1c)$$

Equations 1b or 1c can be used to model any process (such as fatigue crack growth, slow crack growth, stress corrosion etc.) where damage (e.g strain or crack size) has a deceleration to a steady state followed by acceleration when plotted against some suitable determinant (such as time or stress intensity). As such the technique can be applied to various materials undergoing various mechanical or corrosive attacks.

However, in terms of high temperature deformation the first term in Equations 1b and 1c describes normal primary creep and the second term normal tertiary creep. The third term in Equation 1c is a relatively new addition and describes early primary behaviour. As suggested in Evans [9], θ_5 and θ_6 may describe strains that are not permanent so that $\theta_5(1 - e^{-\theta_6 t})$ may be a simple description of anelastic behaviour immediately after loading. It is important to note that the values for θ_1 to θ_4 in Equation 1b will not necessarily be the same as the values for θ_1 to θ_4 in Equation 1c. In principle this representation of strain with time can be applied to any material—metals and plastics alike.

At small strains, the fit of Equation 1b to an experimental creep curves is often very poor, so that for some materials this equation is an inadequate representation of creep. However, for such materials [10, 11] the fit of Equation 1c to the experimental data is very good at low strains. ν_t is a random error term that picks up the experimental errors when measuring strain during a single creep test. That is, ν_t results from experimental inadequacies such as deficiencies in extensometer design, transducers, temperature control and other unexplained effects. These experimental issues inevitably result in values for ν_t being correlated with previous values for ν (e.g. ν_{t-1}) and such autocorrelation has to be accounted for when obtaining estimates for θ_j. Again it should be noted that the values of ν_t in Equations 1b and 1c are not the same.

Values for θ_j are obtained using the method of maximum likelihood [12]. The likelihood function used assumes that ν_t is normally distributed with first order autocorrelation. The precise form of this likelihood function, together with the numerical optimisation procedures used, are described elsewhere [11] and for this paper all the required calculations were implemented within Excel using its Solver Function.

2.2. Projecting a creep curve

For a series of experimental creep curves obtained under different stress conditions, but at a single temperature, the θ_j are related to stress τ by interpolation functions of the form,

$$\theta_j = g_j(\tau, b_{j1}, b_{j2}, \ldots, b_{jk}, \ldots, b_{jp}), \qquad (2a)$$

where the g_j are some linear or more likely non-linear functions, j is a subscript identifying θ in Equation 1a and b_{jp} are constants that need to be determined using a suitable estimation technique. Equation 2a permits the projection of θ_j to new conditions of stress and hence the projection of the complete creep curve to those new conditions. In principle this approach is applicable to all materials.

The following representation for the function g_j in Equation 2a

$$\ln(\theta_j) = b_{j1} + b_{j2}\tau + \sigma_{j1}w_{j1}, \qquad (2b)$$

has been shown to yield excellent predictions of various creep properties including times to moderate and small strains [1–3] in metals. However, different functional forms may work better in other materials, such as plastics and ceramics, and this would constitute a productive area for future research.

σ_{j1}, b_{j1} and b_{j2} are parameters requiring estimation and w_{j1} is a standardised stochastic error term that picks up the variation present in θ_j between those tests performed on the same material at the same test conditions. The first two terms on the right hand side of Equation 2b thus model the variation of θ_j with stress, whilst the last term ($\sigma_{j1}w_{j1}$) models the large variation in θ_j at unchanging test conditions, i.e. at a constant stress. This error, or variation, is likely to be many orders of magnitude larger than the error ν_t contained within a single test. w_{j1} results from microstructural variation from specimen to specimen and possibly variations stemming from the use of different testing machines.

Before Equation 2b can be used to predict, with uncertainty built into this prediction, a creep curve shape at any stress, the nature and properties of w_{j1} must be specified and quantified. Here a generalised log gamma distribution will be used to model the stochastic error w_{j1}. The generalised log gamma distribution takes the following form [13],

$$f(w_{j1}) = \frac{|\lambda_{j1}|}{\Gamma\left(\lambda_{j1}^{-2}\right)}\left(\lambda_{j1}^{-2}\right)^{\lambda_{j1}^{-2}} \exp\left[\lambda_{j1}^{-2}\left(\lambda_{j1}^{-2}w_{j1} - \exp\left(\lambda_{j1}^{-2}w_{j1}\right)\right)\right], \qquad (3a)$$

where $f(w_{j1})$ is the density function for w_{j1} and λ_{j1} is a shape parameter that determines the nature of the distribution for w_{j1}. Γ is the gamma function. Notice that in all cases w_{j1} is a standardised error defined from Equation 2b as

$$w_{j1} = \frac{\ln(\theta_j) - (b_{j1} + b_{j2}\tau)}{\sigma_{j1}}, \qquad (3b)$$

where σ_{j1} are scale parameters that standardises the error w_{j1}. When $\lambda_{j1} = 0$, the w_{j1} follow symmetric normal distributions with means of zero and variances equal to one. Hence it is a standardised error. The term $\exp(w_{j1})$ is therefore log normally distributed. This implies that when $\lambda_{j1} = 0$, the $\ln(\theta_j)$'s follow normal distributions with means equal to $b_{j1} + b_{j2}\tau$, and variances equal to σ_{j1}^2 respectively. When $\lambda_{j1} = 1$, the w_{j1} follow extreme value distributions which skew to the left with means equal to -0.5772 and variances equal to $\pi^2/6$. The term $\exp(w_{j1})$ is therefore Weibull-distributed. This implies that when $\lambda_{j1} = 1$, the $\ln(\theta_j)$'s follow extreme value distributions with means equal to $b_{j1} + b_{j2}\tau - 0.5772\sigma_{1j}$, and variances equal to $(\pi^2\sigma_{j1}^2)/6$. The exponential and gamma distributions are also special cases of this generalised distribution.

The advantage of using this distribution is that it encompasses, as special cases, a variety of distributions including, the Exponential, Weibull, Log Normal and Gamma distributions. As such, a particular type of distribution is not forced upon the data. Rather, the data can be used to determine which of all these distributions best describes the frequency with which various values for the w_{j1} are observed at unchanging test conditions.

The best fitting distribution is defined in terms of the likelihood function, $L(w_{j1}, \lambda_{j1})$, which measures the joint probability of observing each and every w_{j1} value. That is, the distribution that best describes the standardised error w_{1j} is the one with the largest value for $L(w_{j1}, \lambda_{j1})$. This will correspond to a particular value for λ_{j1} so that $L(w_{j1}, \lambda_{j1})$ will be a function of λ_{j1}. It is often simpler to work with the log likelihood function, so that the distribution that best describes w_{j1} is the one with the largest value for $\ln L(w_{j1}, \lambda_{j1})$. From Equation 3a

$$\ln L(w_{j1}, \lambda_{j1}) = n\left[\ln|\lambda_{j1}| - \ln\Gamma\left(\lambda_{j1}^{-2}\right) + \lambda_{j1}^{-2}\ln\left(\lambda_{j1}^{-2}\right)\right] + \sum_{i=1}^{n}\lambda_{j1}^{-2}\left(\lambda_{j1}w_{j1} - \exp\left(\lambda_{j1}w_{j1}\right)\right), \qquad (3c)$$

where n is the number of observations available on $\ln(\theta_j)$.

Values for b_{j1}, b_{j2}, σ_{j1} and λ_{j1} are therefore those values which result in $\ln L(w_{j1}, \lambda_{j1})$ being maximised. These maximum likelihood estimates are asymptotically efficient and the distributions for b_{j1}, b_{j2}, σ_{j1} and λ_{j1} are also asymptotically normal. Moreover, because all the distributions contained within Equation 3a come from the exponential family, if unbiased minimum variance estimators exist, these maximum likelihood estimates will be them [12].

Numerical optimisation procedures for maximising Equation 3c are described elsewhere [14] and for this paper they were implemented within Excel using its Solver Function. This procedure estimates not only the above parameter values but also their standard deviations so that the distributions for all these parameters are fully quantified by this procedure.

It is assumed in this projection technique that λ_{j1} and σ_{j1} are independent of stress. This implies that the distribution for w_{j1} can't be normal at one stress and weibull at another and that the variability in w_{1j}, and thus in $\ln(\theta_j)$, is independent of stress.

2.3. Obtaining a mean creep property prediction

There is more than one way to derive a mean failure time prediction from the theta model described above. The traditional approach has been to find that value for t which satisfies

$$0 = \theta_1(1 - e^{-\theta_2 t}) + \theta_3(e^{\theta_4 t} - 1) - \varepsilon_F, \tag{4a}$$

or in the case of a six theta analysis

$$0 = \theta_1(1 - e^{-\theta_2 t}) + \theta_3(e^{\theta_4 t} - 1) + \theta_5(1 - e^{-\theta_6 t}) - \varepsilon_F. \tag{4b}$$

In Equations 4a and 4b, ε_F is the rupture strain that is in turn related to stress at a single temperature test condition through the formula

$$\varepsilon_F = d_1 + d_2\tau + \sigma_2 w_2, \tag{4c}$$

or

$$w_2 = \frac{\varepsilon_F - (d_1 + d_2\tau)}{\sigma_2}, \tag{4d}$$

where σ_2, and d_1 to d_2 are parameters requiring estimation and w_2 is a standardised stochastic error that picks up the variation in ε_F that is present between a number of tests performed on the same material at the same test conditions. Whilst these equations work well for the creep of metals, other functional forms may be better for plastics and ceramics. Again for modelling purposes w_2 is given a generalised log gamma distribution

$$f(w_2) = \frac{|\lambda_2|}{\Gamma\left(\lambda_2^{-2}\right)}\left(\lambda_2^{-2}\right)^{\lambda_2^{-2}} \exp\left[\lambda_2^{-2}\left(\lambda_2^{-2} w_2 - \exp\left(\lambda_2^{-2} w_2\right)\right)\right]. \tag{5a}$$

Values for d_1, d_2, σ_2 and λ_2 are again those values which result in $\ln L(w_2, \lambda_2)$ being maximised, where

$$\ln L(w_2, \lambda_2) = n\left[\ln|\lambda_2| - \ln\Gamma\left(\lambda_2^{-2}\right)\right) + \lambda_2^{-2}\ln\left(\lambda_2^{-2}\right)\right] + \sum_{i=1}^{n} \lambda_2^{-2}(\lambda_2 w_2 - \exp(\lambda_2 w_2)). \tag{5b}$$

These maximum likelihood estimates are asymptotically efficient and the distributions for d_1, d_2, σ_2 and λ_2 are also asymptotically normal. Numerical optimisation procedures for maximising Equation 5b are described elsewhere [14] and for this paper they were implemented within Excel using its Solver Function. This procedure estimates not only the above parameter values but also their standard deviations so that the distributions for all these parameters are fully quantified.

A mean value for $\ln(\theta_j)$ at any stress τ is then given by

$$\text{Mean}\ln(\theta_j) = \ln(\bar{\theta}_j) = \left[b_{j1} + b_{j2}\tau\right] + \sigma_{j1}\lambda_{j1}^{-1}\left[\Psi\left(\lambda_{j1}^{-2}\right) - \ln\left(\lambda_{j1}^{-2}\right)\right], \tag{6a}$$

with ln variances equal to

$$\text{Variance}\ln(\theta_j) = \sigma_{j1}^2\lambda_{j1}^{-2}\Psi'\left(\lambda_{j1}^{-2}\right). \tag{6b}$$

$\Psi(\lambda_{j1}^{-2})$ and $\Psi'(\lambda_{j1}^{-2})$ are the digamma and trigamma functions respectively and their value depends only on λ_{j1}. (See Lawless [15] for a formal definition of these functions). In addition, for negative values of λ_{j1} the distribution skews to the right so that $-w_{j1}$ has a generalised log gamma distributions with the above means and variances.

Lawless has also shown that the mean and variance for θ_j is then found from

$$\text{Mean}(\theta_j) = \bar{\theta}_j = \frac{\zeta_{j1}\Gamma\left[\left(\zeta_{j2}\lambda_{j1}^{-2} + 1\right)/\zeta_{j2}\right]}{\Gamma\left[\lambda_{j1}^{-2}\right]}, \tag{6c}$$

$$\text{Variance}(\theta_j) = \frac{\zeta_{j1}^2\Gamma\left[\left(\zeta_{j2}\lambda_{j1}^{-2} + 2\right)/\zeta_{j2}\right]}{\Gamma\left[\lambda_{j2}^{-2}\right]} - \left[\frac{\zeta_{j1}\Gamma\left[\left(\zeta_{j2}\lambda_{j1}^{-2}+1\right)/\zeta_{j2}\right]}{\Gamma\left[\lambda_{j1}^{-2}\right]}\right]^2, \tag{6d}$$

where

$$\zeta_{j1} = \exp\left(\left(b_{1j} + b_{2j}\tau\right) - \sigma_{j1}\sqrt{\lambda_{j1}^{-2}}\ln\left(\lambda_{j1}^{-2}\right)\right) \quad \text{and}$$

$$\zeta_{j2} = 1/\left(\sigma_{j1}\sqrt{\lambda_{j1}^{-2}}\right).$$

Similarly, the mean value for ε_F is given by

$$\text{Mean}(\varepsilon_F) = \bar{\varepsilon}_F = [d_1 + d_2\tau] + \sigma_2\lambda_2^{-1}\left[\Psi\left(\lambda_2^{-2}\right) - \ln\left(\lambda_2^{-2}\right)\right], \tag{6e}$$

and the variance for ε_F equals

$$\text{Variance}(\varepsilon_F) = \sigma_2^2\lambda_2^{-2}\Psi'\left(\lambda_2^{-2}\right). \tag{6f}$$

A prediction for the mean creep curve shape at stress τ is found by substituting values for $\bar{\theta}_j$ obtained from Equation 6c into

$$\bar{\varepsilon}_t = \bar{\theta}_1(1 - e^{-\bar{\theta}_2 t}) + \bar{\theta}_3(e^{\bar{\theta}_4 t} - 1) + \bar{\theta}_5(1 - e^{-\bar{\theta}_6 t}). \tag{6g}$$

A prediction of the mean time to failure at any stress τ is found by substituting values for $\bar{\theta}_j$, obtained from Equation 6c, and a value $\bar{\varepsilon}_F$, as given by Equation 6e, into

$$0 = \bar{\theta}_1(1 - e^{-\bar{\theta}_2 t}) + \bar{\theta}_3(e^{\bar{\theta}_4 t} - 1) + \bar{\theta}_5(1 - e^{-\bar{\theta}_6 t}) - \bar{\varepsilon}_F, \tag{6h}$$

and solving for t.

The disadvantage of this approach is that for most metallic materials ε_F is not strongly dependant on stress or temperature. Whilst this tends to lead to errors in failure time predictions it should be noted that this transmitted error is minimised by the fact that the creep curve is at its steepest close to the time of failure.

A second approach is to combine the above theta analysis with the Monkman–Grant relation [16] that stipulates that the time to failure is inversely proportional to the minimum creep rate ε_M,

$$\ln(t_F) = \ln(\alpha) + \beta\ln(\varepsilon_M) + \sigma_3 w_3; \quad \beta < 0, \tag{7a}$$

where α, β and σ_3 are constants that can be estimated from the test matrix data set using maximum likelihood procedures and w_3 is standardised stochastic error. Again for modelling purposes w_3 is given a generalised log gamma distribution

$$f(w_3) = \frac{|\lambda_3|}{\Gamma\left(\lambda_3^{-2}\right)}\left(\lambda_3^{-2}\right)^{\lambda_3^{-2}} \times \exp\left[\lambda_3^{-2}\left(\lambda_3^{-2} w_3 - \exp\left(\lambda_3^{-2} w_3\right)\right)\right]. \quad (7b)$$

Values for α, β, σ_3 and λ_3 are again those values which result in $\ln L(w_3, \lambda_3)$ being maximised where

$$\ln L(w_3, \lambda_3) = n\left[\ln|\lambda_3| - \ln\Gamma\left(\lambda_3^{-2}\right)\right) + \lambda_3^{-2}\ln\left(\lambda_3^{-2}\right)\right] + \sum_{i=1}^{n} \lambda_3^{-2}(\lambda_3 w_3 - \exp(\lambda_3 w_3)). \quad (7c)$$

These maximum likelihood estimates are asymptotically efficient and the distributions for α, β, σ_3 and λ_3 are also asymptotically normal. Numerical optimisation procedures for maximising Equation 7c are described elsewhere [14] and for this paper they were implemented within Excel using its Solver Function. This procedure estimates not only the above parameter values but also their standard deviations so that the distributions for all these parameters are fully quantified.

In turn the theta analysis suggests that the minimum creep rate is given by

$$\dot{\varepsilon}_M = -\theta_1\theta_2\, e^{-\theta_2 t_M} + \theta_3\theta_4\, e^{\theta_4 t_M}, \quad (8a)$$

or if six theta parameters are used, by

$$\dot{\varepsilon}_M = -\theta_1\theta_2\, e^{-\theta_2 t_M} + \theta_3\theta_4\, e^{\theta_4 t_M} - \theta_5\theta_6\, e^{-\theta_6 t_M}. \quad (8b)$$

In each of the above equations t_M is the time to minimum creep rate. When using four theta parameters

$$t_M = \frac{1}{\theta_2 + \theta_4}\ln\frac{\theta_1\theta_2^2}{\theta_3\theta_4^2}, \quad (8c)$$

and in the case of six theta parameters t_M is given by the value for t that satisfies Equation 8d below

$$\frac{\theta_1\theta_2^2}{\theta_3\theta_4^2}\, e^{t[-\theta_2-\theta_4]} + \frac{\theta_5\theta_6^2}{\theta_3\theta_4^2}\, e^{t[-\theta_6-\theta_4]} - 1 = 0. \quad (8d)$$

The mean minimum creep rate, $\dot{\bar{\varepsilon}}_M$ at any stress τ is found by replacing θ_j in Equations 8a or 8b with the mean θ_j values given by Equation 6c. The mean value for $\ln(t_F)$ therefore equals

$$\text{Mean}\ln(t_F) = \ln(\bar{t}_F) = [\alpha + \beta\ \ln(\dot{\bar{\varepsilon}}_M)] + \sigma_3\lambda_3^{-1}\left[\Psi\left(\lambda_3^{-2}\right) - \ln\left(\lambda_3^{-2}\right)\right], \quad (8e)$$

where $\dot{\bar{\varepsilon}}_M$ is the mean minimum creep rate at stress τ. The variance for $\ln(t_F)$ is then given by

$$\text{Variance}\ln(t_F) = \sigma_3^2\lambda_3^{-2}\Psi'\left(\lambda_3^{-2}\right). \quad (8f)$$

2.4. Obtaining a creep property prediction with confidence using Monte Carlo simulation

In the previous section the stochastic variables w_{j1}, w_2 and w_3 were modelled as generalised log gamma distributions whilst the variables α, β, b_{j1}, b_{j2}, d_1, d_2, λ_1, λ_2, λ_3, σ_{j1}, σ_2 and σ_3 were modelled as normal distributions. These stochastic variables, together with the stress level are the major determinants of a creep property prediction.

To go from a mean value prediction of the time to failure to a distribution of failure times a closer look at the determinants of time to failure in the two models specified in the last section is required. In the approach that uses a rupture strain relation the fundamental determinants of time to failure are b_{j1} and b_{j2}, σ_{j1}, w_{j1}, d_1, d_2, σ_2 and w_2. In the approach that uses the Monkman–Grant relation, the fundamental determinants of time to failure are b_{j1} and b_{j2}, σ_{j1}, w_{j1}, α, β, σ_3 and w_3.

More importantly, the above analysis has shown that these determinants are stochastic and the distributions identified above for each of these determinants, as quantified using the maximum likelihood method described above, can be used to compute an empirical failure time distribution at any stress. In particular, it is required to sample values from each of these distributions. Here Latin Hyper Cube sampling has been used in which the distributions of each failure time determinant are divided into equal intervals and a sample value is then randomly taken from each interval. The number of intervals is equal to the number of iterations used and here it is equal to 2500. This stratified approach allows a more accurate recreation to be made of the distributions when using fewer iterations compared to a standard Monte Carlo technique.

Latin Hyper Cube sampling was carried out within Excel using the @Risk Addin [17]. This Addin creates, at random, a number between 0 and 1 for each failure time determinant highlighted above using a random number generator. These can be considered as the cumulative probabilities of observing each of the determinants defined above. For variables w_{j1} these cumulative probabilities are first converted into variables, z_{j1}, that follow a one parameter gamma distribution—that is a gamma distributions with a scale parameters of 1 and a shape parameters given by λ_{j1}. w_{j1} is then given as

$$w_{j1} = \lambda_{j1}^{-1}\left[\ln(z_{j1} - \ln\left(\lambda_{j1}^{-2}\right)\right]. \quad (9a)$$

Similarly, values for w_2 and w_3 were obtained as

$$w_2 = \lambda_2^{-1}\left[\ln(z_2 - \ln\left(\lambda_2^{-2}\right)\right], \quad (9b)$$

$$w_3 = \lambda_3^{-1}\left[\ln(z_3 - \ln\left(\lambda_3^{-2}\right)\right] \quad (9c)$$

Repeating this process leads to a series of values for each of the failure time determinants that have a generalised log gamma distribution. Parameters b_{j1} and b_{j2}, σ_{j1}, d_1, d_2, σ_2 and, α, β, and σ_3 will be estimated using maximum likelihood techniques and so are asymptotically normally distributed with zero means and various standard deviations. As such, values for these variables can be obtained from a set of random numbers between 0 and 1. These are the cumulative

probabilities associated with these variables and their associated standardised z values are therefore read off from a standard normal distribution table. These Z values are then converted into un standardised values (i.e. values for b_{j1} etc) using the means and standard deviations for each variable. When carrying out such sampling any strong dependencies between b_{j1} and b_{j2} need to be taken into account.

A distribution for the predicted failure time associated with a particular stress level can now be found. When using the rupture strain relation a value for b_{j1}, $b_{j2}, \sigma_{j1}, \sigma_2, d_1, d_2, w_{j1}$ and w_2 is sampled (using Latin Hypercube sampling) from their respective distributions. The sampled values for b_{j1} and b_{j2}, σ_{j1} and w_{j1} are substituted into Equation 2b, together with a value for the required stress τ, to derive a value for $\ln(\theta_j)$. Then the sampled values for d_1 and d_2, σ_2 and w_2, together with a value for the required stress τ, are substituted into Equation 4c to derive a value for ε_F. These values for (θ_j) and ε_F are then substituted into Equations 4a and 4b and these equations are then solved numerically to find a predicted failure time using the four theta and six theta approaches. These calculations are then repeated another 2499 times to give a total of 2500 failure times using the four and six theta techniques. From such a large number of failure times a simple histogram or empirical failure time distribution can be constructed.

When using the Monkman–Grant relation a value for $b_{j1}, b_{j2}, \sigma_{j1}, \sigma_3, \alpha, \beta, w_{j1}$ and w_3 is sampled (using Latin Hypercube sampling) from their respective distributions. The sampled values for b_{j1} and b_{j2}, σ_{j1} and w_{j1} are substituted into Equation 2b, together with a value for the required stress τ, to derive values for $\ln(\theta_j)$. Next these values for (θ_j) are substituted into Equations 8a to 8d to obtain a prediction of the minimum creep rate using four and six theta values. Then, the sampled values for α, β, σ_3 and w_3 together with the predicted ln minimum creep rate are substituted into Equation 7a to derive a value for $\ln(t_F)$. These calculations are then repeated another 2499 times to give a total of 2500 ln failure times using the four and six theta techniques.

With 2500 values for time to failure and its determinants it is possible to see which of these determinants are the most important by carrying out a simple linear regression. When using a rupture strain relation this regression equation takes the form

$$\ln(t_F)_i = \delta_0 + \delta_1 \varepsilon_{F_i} + \delta_j \sum_{j=2}^{5 \text{ or } 7} \ln(\theta_j)_i + \zeta_i. \quad (10a)$$

where there are $i = 1$ to 2500 values for each variable in Equation 10a and δ_0, δ_1 and δ_j are parameters to be estimated using the least squares technique—by minimising the sum of squared errors $-\sum_{i=1}^{2500} \zeta_i^2$. Notice that the determinants $w_{j1}, b_{j1}, b_{j2}, \sigma_{j1}$ have been combined into each θ_j value and values for d_1, d_2, σ_2 and w_2 have been combined into each ε_F value. When using the Monkman–Grant relation this regression equation takes the form

$$\ln(t_F)_i = \delta_0 + \delta_1 \beta_1 + \delta_2 \sigma_{2i} + \delta_j \sum_{j=3}^{6 \text{ or } 8} \ln(\theta_j)_i + \xi_i. \quad (10b)$$

The size of each δ value, together with the simple correlation coefficient between log time to failure and the right hand side variables in Equation 10a and 10b is then an indication of the importance of each determinant of failure time. Another indicator is the squared partial correlation coefficient that measures the proportion of the variation in ln time to failure, not explained by all but one of the right hand side variables in Equations 10a and 10b which is explained by adding the remaining variable to Equations 7a and 7b. (See Thomas [18] for more details on its derivation).

3. Modification of stochastic theta model for fatigue data

When using the above theta model to analysis failure under fatigue conditions, two approaches can be taken. The first approach involves very little alteration to what has been said above. Here crack growth is totally ignored and instead strain is used. Even under a cyclical stress at room temperature strain accumulation will occur. This strain can be analysed in exactly the same way as a creep strain. This approach was adopted by Bache and Evans [19] using a non stochastic four theta approach, i.e. the above model with the variances for $b_{j1}, b_{j2}, \sigma_{j1}, \sigma_2, d_1, d_2, w_{j1}$ and w_2 all equal to zero.

The second approach is to work with a plot of crack growth per cycle, against the cyclic stress intensity factor and model this relationship using a four of six theta equation,

$$\frac{da}{dN} = \theta_1(1 - e^{-\theta_2 \Delta K}) + \theta_3(e^{\theta_4 \Delta K} - 1) + \nu, \quad (11a)$$

or,

$$\frac{da}{dN} = \theta_1(1 - e^{-\theta_2 \Delta K}) + \theta_3(e^{\theta_4 \Delta K} - 1) + \theta_5(1 - e^{-\theta_6 \Delta K}) + \nu, \quad (11b)$$

where a is crack length, N is the number of stress cycles, ΔK is the cyclic stress intensity factor and da/dN the crack growth per cycle. This can be though of as a generalisation of the Paris and Erdogan [20] equation

$$\frac{da}{dN} = A \Delta K^m, \quad (11c)$$

where A and m are constants. This equation however is only valid over the steady state range. The number of cycles, N_0, to a given crack length, a_0, can then be worked out by solving

$$N_0 = \int_0^{N_0} dN = \int_0^{a_0} \frac{da}{\theta_1(1 - e^{-\theta_2 \Delta K}) + \theta_3(e^{\theta_4 \Delta K} - 1) + \theta_5(1 - e^{-\theta_6 \Delta K})}, \quad (11d)$$

for a six theta approach. If the relationship between tests conditions and crack length at rupture exists this can be built into Equation 11d and the number of cycles to

rupture predicted. To the author's best knowledge this approach has not yet been tried out.

4. Experimental procedures

The material used in this investigation is titanium alloy Ti-6.2.4.6 prepared as an ingot forged in the β-phase at approximately 1238 K (the β transus is approximately 1223 K). The chemical composition of this material (in wt%) was determined as 5.79 A1, 1.99 Sn, 3.94 Zr, 6.03 Mo, 0.06 Fe, 0.02 C, 0.1 O, 0.0035 Si and Balance $\sim$ 82 Ti. The initial heat treatment schedule used was 1173 K for two hours, followed by air quenching. It was then reheated to 868 K, held for eight hours, and finally air quenched. A second re-age for two hours at 913 K, in air, was employed, which is a simulated post weld heat treatment.

Twenty-three conventional creep specimens, from material supplied by TIMET U.K. Ltd., of 3.8 mm diameter, 25.4 mm gauge length and 3/8 inch BSF thread were machined from the heat treated material and tested in tension over a range of stresses at 773 K using seven high precision uniaxial constant-stress machines fitted with three zone furnaces. All machines had been calibrated to British Standards BSEN10002 (parts 1–5). Details of such testing machines can be found in most texts on creep [21]. Temperature was maintained along the gauge length and with respect to time to better than ± 0.5 K and the extensometers were capable of establishing creep strains to better than 10^{-5} and the creep strain-time curves contained approximately 400 points. Digital data collection was used in all cases.

The test matrix used is summarised in Table I. Fifteen of the twenty-three specimens were placed on test at 773 K and a stress of 580 MPa, with the remaining eight specimens being tested at 773 K and over the stress range 900 MPa to 480 MPa—excluding 580 MPa. The creep properties contained in this table have been reported (in part) elsewhere [22]. The test matrix has fifteen specimens placed on test at a single condition (773 K and 580 MPa) so that reliable estimates can be made of the distributions of the failure time determinants.

5. Results

5.1. Fitting creep curves using estimated theta values

Table II shows the results obtained from estimating Equations 1b and 1c for all the different test conditions shown in Table I. As each theta value is quite small, and as the log of each theta value is linearly related to stress, the natural log of these theta values are shown. Note how the values for $\ln(\theta_1)$ to $\ln(\theta_4)$ are similar but not exactly the same in each equation. Notice also the substantial scatter in the $\ln(\theta_j)$ estimates over the 15 tests at 580 MPa. Fig. 1a shows the different types of fit given by Equations 1b and 1c to the experimental creep curve obtained at 535 MPa. Note how the fit given by Equation 1c, that uses six theta values, is better than that obtained from using Equation 1b—especially over the low strain range.

Fig. 1b gives a more complete view of the creep curves obtained for the test matrix defined in section 4 above. In Fig. 1b, only two creep curves from the 15 available at the repeat stress of 580 MPa and 773 K are shown and they correspond to the maximum and minimum rupture times at this test condition. Also shown are some creep curves obtained at different stresses together with the experimental strain points around the fitted curve (using six theta values) at 535 MPa.

Fig. 1b clearly reveals that any successful prediction technique must be able to model both the changing form of the creep curves with stress and the huge variability present in the form of the creep curves at an unchanging stress (e.g. at 580 MPa). Creep curves obtained at stresses other than 580 MPa fall within the range of creep curves obtained at 580 MPa. Indeed this latter property is so significant that it dwarfs the size of ν_t, shown in Fig. 1b, by the small deviation of points around the fitted creep curve at 535 MPa. So whilst each θ_j obtained from a single test is itself stochastic, this variability is dwarfed by the variations in θ_j observed from test to test and this latter variability needs to be modelled accurately if a reliable failure time distribution is to be obtained.

5.2. Theta projection equations and theta distributions

Table III shows the results obtained from estimating the parameters in Equation 2b through the maximisation of Equation 3c for each θ_j value. The top half of the table shows the estimates made of Equation 2b when four theta values were used to represent the form of the creep curve and the bottom half of the table shows the estimates made of Equation 2b when six theta values were used. A number of interesting points emerge. Most important is the realisation that each $\ln(\theta_j)$ value has a different shaped distribution. When using four theta values, $\ln(\theta_1)$ and $\ln(\theta_3)$ are approximately normally

TABLE I Isothermal (773 K) testing matrix showing the number of specimens tested on various machines and at various stresses

Stress (MPa)	Machine 1	Machine 2	Machine 3	Machine 4	Machine 5	Machine 6	Machine 7
900			1				
800			1				
700						1	
620		1					
600							1
580	3	3	3	3	3		
560				1			
535							1
480					1		

TABLE II Theta values obtained by fitting Equations 1b and 1c using maximum likelihood

Stress (MPa)	$\ln(\theta_1)$	$\ln(\theta_2)$	$\ln(\theta_3)$	$\ln(\theta_4)$	$\ln(\theta_5)$	$\ln(\theta_6)$
480	−4.97577	−11.8958	−2.74229	−16.6852	–	–
	−4.3863	−15.0179	−4.09226	−15.9257	−5.36426	−10.9049
535	−4.45792	−12.287	−3.3996	−15.1233	–	–
	−1.27161	−16.9244	−5.89481	−14.3884	−4.99867	−10.8389
560	−4.8652	−10.6883	−2.49825	−15.0035	–	–
	−5.06766	−12.0475	−2.85737	−14.7747	−5.53312	−9.44909
600	−4.58348	−11.4117	−3.02412	−15.0212	–	–
	−4.82096	−11.4797	−2.79317	−14.8472	−5.83451	−8.39626
620	−4.82947	−10.1097	−2.28751	−15.1903	–	–
	−3.56997	−13.2123	−4.04868	−13.6405	−5.21108	−9.25547
700	−4.50018	−10.5904	−2.84086	−14.1811	–	–
	−3.46257	−12.8063	−3.89631	−13.0229	−4.67338	−9.40116
800	−4.28971	−10.2048	−2.65126	−13.6029	–	–
	−3.36686	−11.0852	−3.23494	−12.0332	−4.65171	−8.13346
900	−3.92549	−9.30924	−2.02357	−12.6859	–	–
	−3.54816	−8.94833	−3.37953	−10.3995	−5.3255	−6.01207
580	−4.7111	−10.555	−2.7881	−14.7388	–	–
	−4.83688	−12.1075	−3.06287	−14.5778	−5.68021	−8.86962
580	−4.4062	−10.4604	−2.38075	−15.4334	–	–
	−4.59273	−12.6154	−3.0571	−14.9978	−5.00112	−9.22643
580	−4.57893	−10.5066	−2.94129	−14.8724	–	–
	−4.49706	−13.0563	−3.48434	−14.5933	−5.20086	−9.16617
580	−4.49786	−11.0961	−3.18508	−14.5875	–	–
	−4.16912	−13.3114	−3.83986	−14.2912	−5.22198	−9.65152
580	−4.46793	−12.1769	−3.58606	−14.7559	–	–
	−2.20154	−15.6269	−6.09075	−14.0073	−5.31718	−9.90936
580	−4.6969	−11.3583	−3.33171	−15.0849	–	–
	−4.49966	−13.4922	−4.15177	−14.678	−5.32799	−9.79919
580	−4.38082	−11.3964	−2.92662	−14.6829	–	–
	−3.77963	−13.7041	−3.6348	−14.3752	−5.13801	−9.5614
580	−4.28615	−11.9447	−3.48024	−14.801	–	–
	−3.14354	−14.7223	−4.97172	−14.2778	−4.90661	−10.4234
580	−4.61547	−11.8612	−3.41847	−15.0275	–	–
	−4.48553	−13.5605	−4.03772	−14.7327	−5.34175	−9.82821
580	−4.53832	−11.5053	−3.22329	−14.7588	–	–
	−4.69313	−12.9656	−3.5472	−14.5977	−5.25584	−9.38131
580	−4.69574	−11.6496	−2.70027	−15.8015	–	–
	−4.88315	−13.1942	−3.1691	−15.5003	−5.44831	−9.92599
580	−4.92178	−11.3377	−2.89925	−15.1794	–	–
	−4.8118	−13.2895	−3.47322	−14.8552	−5.49938	−10.2004
580	−4.80743	−11.4196	−2.57967	−15.4894	–	–
	−4.55649	−13.5283	−3.44358	−14.9718	−5.34637	−10.2095
580	−4.65537	−11.8031	−3.00716	−15.0792	–	–
	−4.82417	−13.1734	−3.26522	−14.9449	−5.36645	−10.0286
580	−4.49221	−12.1042	−2.91376	−15.0259	–	–
	−2.8128	−15.0291	−4.48566	−14.4165	−5.04114	−10.55

Estimates of Equation 1b are shown in the first line associated with each stress and Equation 1c in the second line.

TABLE III Maximum likelihood estimates of the parameters in Equation 2b

	$\ln(\theta_1)$	$\ln(\theta_2)$	$\ln(\theta_3)$	$\ln(\theta_4)$	$\ln(\theta_5)$	$\ln(\theta_6)$
λ_{j1}	0.05	−0.8	−0.01	1.282	–	–
b_{j1}	−5.9789	−17.733	−4.8291	−20.8808	–	–
b_{j2}	0.00237	0.01071	0.00327	0.01056	–	–
σ_{j1}	0.16852	0.48106	0.34811	0.18210	–	–
λ_{j1}	−1.826	0.6	1.826	0.1	0.7	−0.7
b_{j1}	−6.8927	−20.4750	−3.1667	−21.8416	−6.1572	−15.5069
b_{j2}	0.00385	0.01247	−0.00015	0.01252	0.00166	0.00959
σ_{j1}	0.39159	0.98651	0.44153	0.36565	0.24015	0.48538

θ_j is the jth theta relation (Equation (2b), λ_{j1} is the distributions shape parameter for each theta, σ_{j1} the distributions scale parameter for each theta and β_{j1} are the distribution location parameters that relate each theta to stress.

distributed as shown by the λ_{j1} values being close to zero. However, $\ln(\theta_2)$ has a long tail towards larger θ_2 values (as shown by a large negative value for λ_{21}) whilst $\ln(\theta_4)$ has an even longer tail towards smaller θ_4 values (as shown by a large positive value for λ_{41}). This is more clearly seen in Figs. 2a and 2b which show the distributions for $\ln(\theta_2)$ and $\ln(\theta_4)$ respectively.

When using six theta values, $\ln(\theta_4)$ is approximately normally distributed as shown by a λ_{41} value close to zero. However, $\ln(\theta_2)$, $\ln(\theta_5)$ have similar generalised

TABLE IV Variance–covariance matrix for the parameters in Equation 2b

	$\ln(\theta_1)$			$\ln(\theta_2)$			$\ln(\theta_3)$			$\ln(\theta_4)$		
	b_{j1}	b_{j2}	σ_{j1}	b_{j1}	b_{j2}	σ_{j1}	b_{j1}	b_{j2}	σ_{j1}	b_{j1}	b_{j2}	σ_{j1}
b_{j1}	0.252	−0.990	−0.001	0.767	−0.991	0.011	0.0522	−0.990	0.002	0.284	−0.989	0.137
b_{j2}	−0.990	0.0004	0.0003	−0.991	0.0013	−0.089	−0.990	0.001	−0.001	−0.989	0.001	0.077
σ_{j1}	−0.001	0.0003	0.025	0.011	−0.089	0.077	0.002	−0.001	0.051	0.137	0.077	0.034

	$\ln(\theta_1)$			$\ln(\theta_2)$			$\ln(\theta_3)$		
	b_{j1}	b_{j2}	σ_{j1}	b_{j1}	b_{j2}	σ_{j1}	b_{j1}	b_{j2}	σ_{j1}
b_{j1}	0.573	−0.988	0.113	1.500	−0.99	−0.083	0.762	−0.991	−0.912
b_{j2}	−0.988	0.001	−0.059	−0.990	0.003	0.055	−0.991	0.001	0.136
σ_{j1}	0.113	−0.059	0.076	−0.083	0.055	0.152	−0.192	0.136	0.081

	$\ln(\theta_4)$			$\ln(\theta_5)$			$\ln(\theta_6)$		
	b_{j1}	b_{j2}	σ_{j1}	b_{j1}	b_{j2}	σ_{j1}	b_{j1}	b_{j2}	σ_{j1}
b_{j1}	0.542	−0.99	−0.015	0.398	−0.992	0.083	0.788	−0.991	−0.025
b_{j2}	−0.990	0.001	0.010	−0.992	0.001	−0.114	−0.991	0.001	0.056
σ_{j1}	−0.015	0.010	0.054	0.083	−0.114	0.038	−0.025	0.056	0.077

The estimated standard for each parameter of Equation 2b are shown down the diagonals of each theta column and the correlation coefficients between each parameter are shown in the off diagonals. The top third of the table is for a four theta analysis, the bottom two thirds for a six theta analysis.

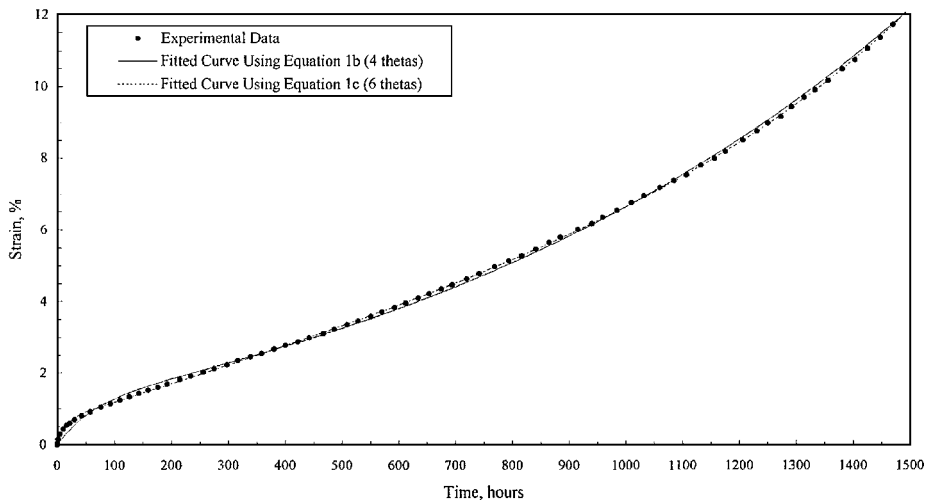

(a)

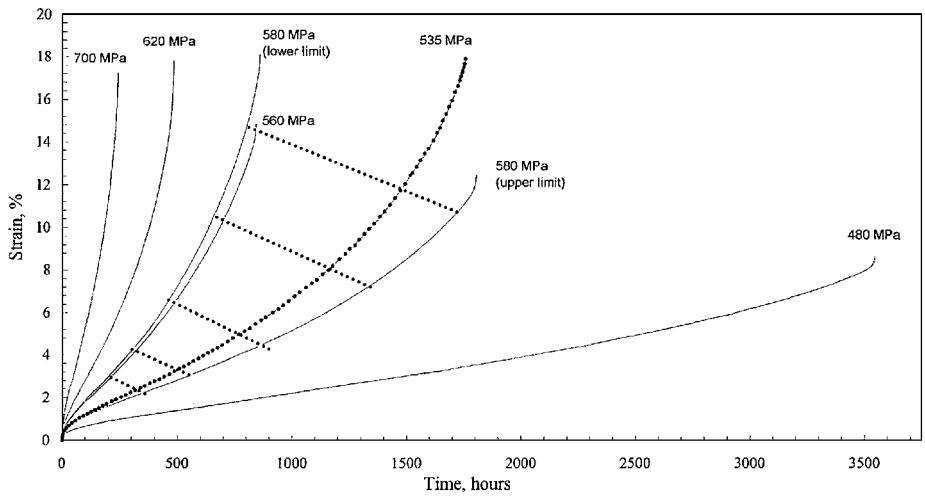

(b)

Figure 1 (a) Uniaxial experimenttal creep curve at 535 MPa and 773 K for Ti-6.2.4.6 together with curves fitted using Equation 1b and 1c. (b) Uniaxial creep curves at 773 K for Ti-6.2.4.6 (including the band of the creep curves obtained at a repeat stress of 580 MPa bounded by the maximum and minimum rupture times).

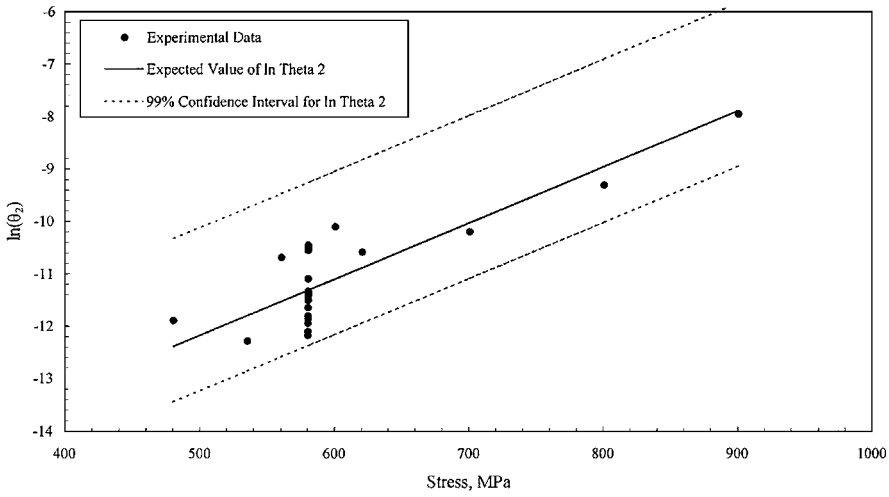

(a)

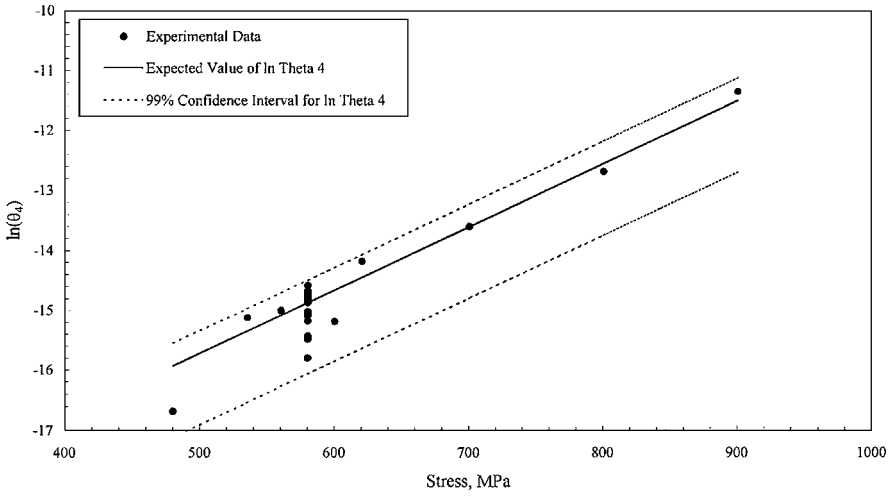

(b)

Figure 2 (a) Distribution for $\ln(\theta_2)$ when using Equation 1b to represent an experimental creep curve. (b) Distribution for $\ln(\theta_4)$ when using Equation 1c to represent an experimental creep curve.

log gamma representations with moderate length tails to the left of the peak point of their distributions. $\ln(\theta_1)$ and $\ln(\theta_6)$ have long tails to the right of their peak points, whilst $\ln(\theta_3)$ has an even longer tail to the left of its peak point.

Equation 6b makes clear the fact that σ_{j1} is a strong measure of the variability present between each $\ln(\theta_j)$ estimate (indeed when $\lambda_{j1} = 0\,\sigma_{j1}$ are the standard deviations themselves). It can be seen from Table III that when using four theta values, $\ln(\theta_2)$ has the most scatter and $\ln(\theta_4)$ the least—this again is clearly visible from a comparison of Figs. 2a and 2b. When using six theta values, $\ln(\theta_2)$ has the most scatter and $\ln(\theta_4)$ and $\ln(\theta_5)$ the least. Table IV shows the correlation coefficient between each of the parameters of Equation 2b. They suggest that the coefficients b_{j1} and b_{j2} are very dependant, whilst b_{j1} and σ_{j1} and b_{j2} and σ_{j1} are broadly independent. This dependency must be taken into account when deriving the failure time distributions below.

5.3. Estimation of failure criteria and mean times to failure

The results of estimating the parameters in Equation 4c are shown in the left hand side of Table V. Table VI contains the standard deviations of these parameter estimates and as expected the parameter d_2 is statistically

TABLE V Maximum likelihood estimates of the parameters in Equations 4c and 7a

	ε_F		$\ln(t_F)$
λ_2	−0.02	λ_3	0.9
d_1	0.1494	α	−0.4551
d_2	0.00003	β	−0.8869
σ_2	0.0450	σ_3	0.1404

ε_F is the rupture strain relation (Equation 4c), $\ln(t_F)$ the log time to failure in the Monkman–Grant relation (Equation 5a), λ_2 and λ_3 is the distribution shape parameters for ε_F and $\ln(t_F)$ respectively, σ_2 and σ_3 the distribution scale parameters for ε_F and $\ln(t_F)$, d_1 and d_2 are the distribution location parameters that relate ε_F to stress and α and β are the distribution location parameters that relate $\ln(t_F)$ to the ln minimum creep rate, ε_M

TABLE VI Variance–covariance matrix for the parameters in Equations 4c and 7a

	ε_F			$\ln(t_F)$		
	d_1	d_2	σ_2	d_1	d_2	σ_2
d_1	0.0628	−0.0989	0.0269	0.06058	0.9987	−0.0673
d_2	−0.0989	0.0001	−0.0167	0.9987	0.0349	−0.0528
σ_2	0.0269	−0.0167	0.0067	−0.0673	−0.0528	0.0225

The estimated standard deviation for each parameter of Equations 4c and 7a are shown down the diagonals of the ε_F and $\ln(t_F)$ columns and the correlation coefficients between each parameter are shown in the off diagonals.

insignificant and the closeness of λ_2 to zero suggests that the distribution for ε_f is also normal with a standard deviation of $\sigma_2 = 0.045$. A mean or expected time to failure at a particular stress can now be obtained as follows. Use Equation 6c together with the required values shown in Table III to obtain an expected value for each (θ_j). Next use Equation 6e together with the required values shown in Table V to obtain an expected value for ε_F. Then substitute these mean values for (θ_j) and ε_F into Equation 6h and solve numerically for an expected failure time. A four theta approach can also be used. A mean creep curve can be found by substituting the mean values for (θ_j) and ε_F into Equation 6g.

As an illustration take the stresses 580 MPa and 480 MPa. Using four theta values, this approach predicts a mean failure time at 580 MPa of 1364 hours and

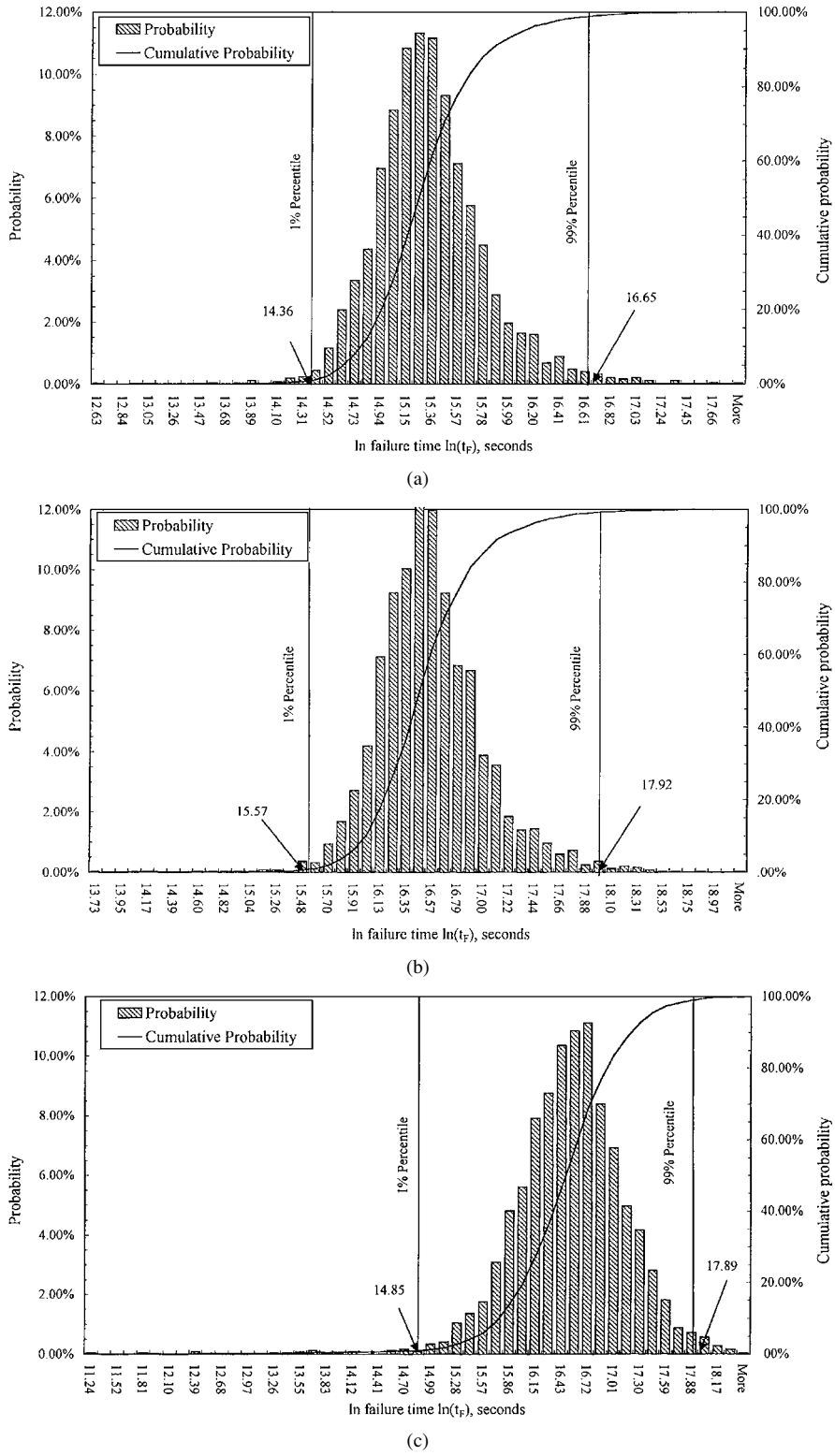

Figure 3 (a) The ln failure time distribution at 580 MPa obtained by using the rupture strain failure criteria and Equation 1b to represent an experimental creep curve. (b) The ln failure time distribution at 480 MPa obtained by using the rupture strain failure criteria and Equation 1b to represent an experimental creep curve. (c) The ln failure time distribution at 580 MPa obtained by using the rupture strain failure criteria and Equation 1c to represent an experimental creep curve.

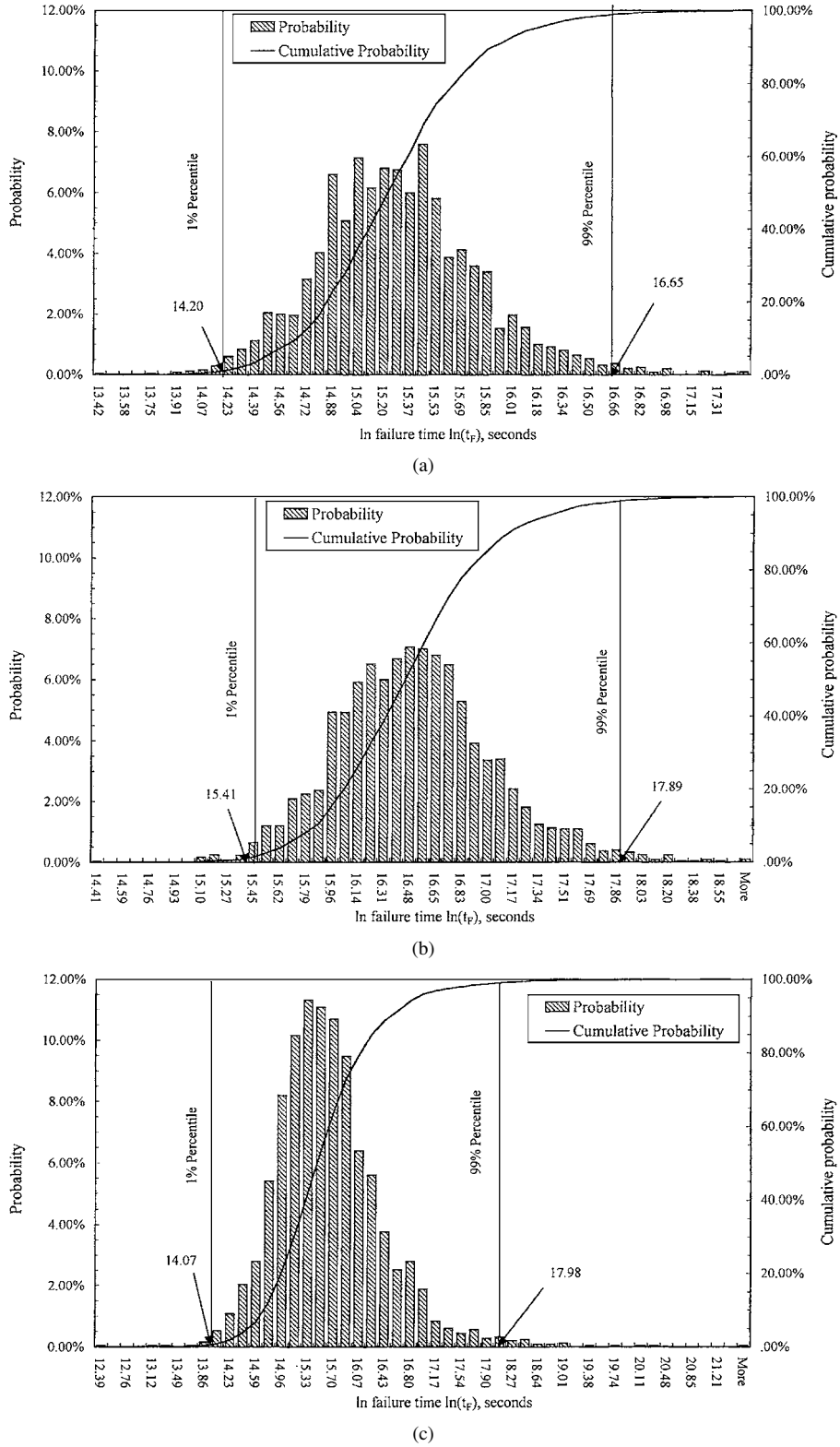

Figure 4 (a) The ln failure time distribution at 580 MPa obtained by using the Monkman–Grant failure criteria and Equation 1b to represent an experimental creep curve. (b) The ln failure time distribution at 480 MPa obtained by using the Monkman–Grant failure criteria and Equation 1b to represent an experimental creep curve. (c) The ln failure time distribution at 580 MPa obtained by using the Monkman–Grant failure criteria and Equation 1c to represent an experimental creep curve.

at 480 MPa 4614 hours. Using the six theta approach, a mean failure time at 580 MPa of 1316 hours is predicted and at 480 MPa a life of 4664 hours is predicted. The four and six theta approaches therefore give very similar mean failure times and this will be further confirmed below.

The results of estimating the parameters in Equation 7a are shown in the right hand side of Table V. The standard deviations shown in Table VI suggested that the parameter β is statistically significant but α is not and so is set equal to zero in all subsequent analysis. The value of λ_3 suggests that the distribution for $\ln(t_F)$ is skewed to the left. A mean or expected time to failure at a particular stress can now be obtained as follows. Use Equation 6c together with the required values shown in Table III to obtain an expected value for each (θ_j).

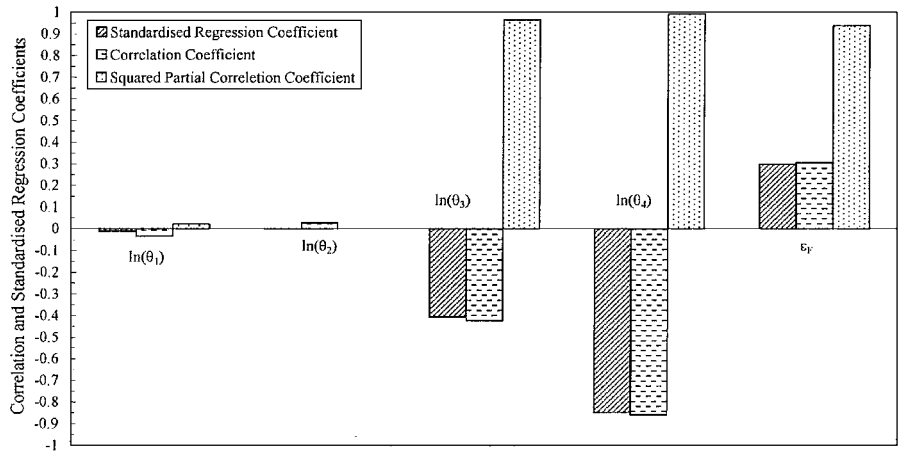

(a)

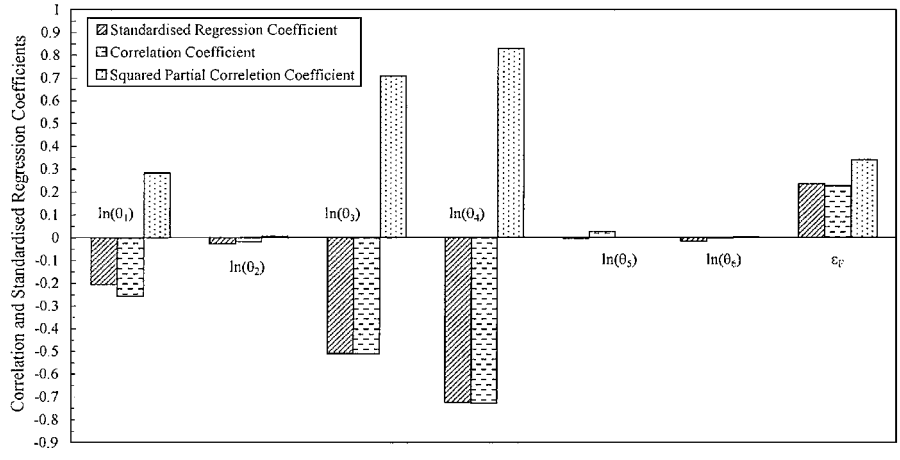

(b)

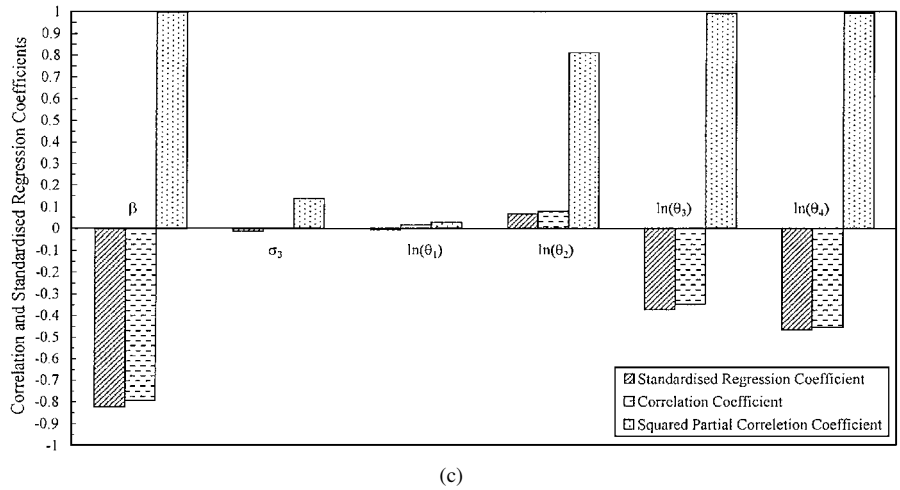

(c)

Figure 5 (a) Sensitivity of ln time to failure to its determinants obtained when the rupture strain failure criteria and Equation 1b represent an experimental creep curve. (b) Sensitivity of ln time to failure to its determinants obtained when the rupture strain failure criteria and Equation 1c represent an experimental creep curve. (c) Sensitivity of ln time to failure to its determinants obtained when the Monkman–Grant failure criteria and Equation 1b represent an experimental creep curve. (d) Sensitivity of ln time to failure to its determinants obtained when the Monkman–Grant failure criteria and Equation 1c represent an experimental creep curve. (*Continued*.)

Next, substitute these mean values into Equations 8a to 8d and solve, numerically in the case of a six theta analysis, for the mean minimum creep rate. Then substitute this mean minimum creep rate prediction into Equations 8e to obtain a mean ln time to failure.

Using four theta values this approach predicts a mean failure time at 580 MPa of 1344 hours and at 480 MPa a life of 4590 hours is predicted. Using the six theta approach a mean failure time at 580 MPa of 1575 hours is predicted and at 480 MPa a life of 5111 hours is predicted.

When using four theta values, the two approaches (using a rupture strain or the Monkman–Grant relation) predict very similar mean times to failure. However, when six thetas are used the Monkman–Grant approach predicts a much higher mean value at the two stresses shown. These numbers represent a prediction for the mean life of this alloy when operating at these stresses and temperatures under uniaxial conditions. They do not represent a life expectancy of a titanium turbine blade or disk because such components are subjected to varying stresses and temperatures and to multiaxial

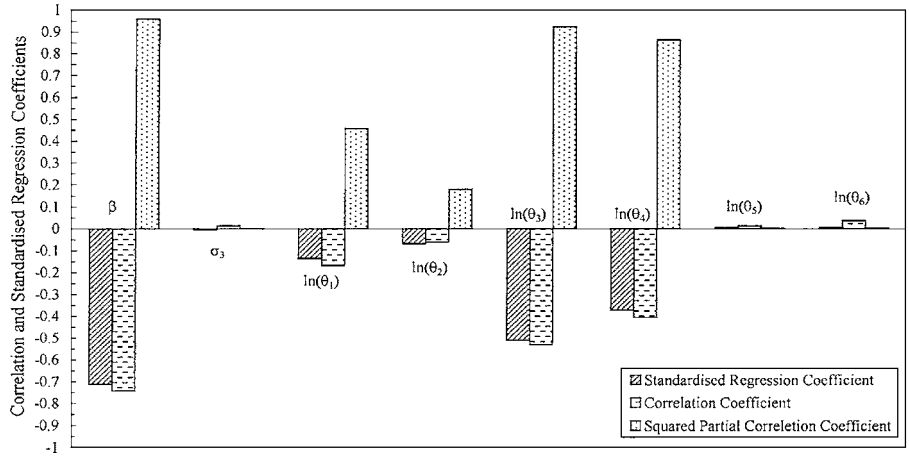

(d)

Figure 5 (*Continued*).

loadings. Extending the theta model to deal with such a situation is the next big challenge.

5.4. Monte Carlo derivation of some empirical failure time distributions

Figs 3a–c show some distributions for the predicted time to failure at various stresses under uniaxial loading using the rupture strain failure criteria. They were obtained in the way described in Section 2.4 above. Fig. 3a shows the failure time distribution predicted for a stress of 580 MPa derived using four theta values. Note that the failure time associated with the peak point of this distribution is similar to the mean value derived in the previous section. Of more interest however is the lower bound of this distribution showing that there is only a 1% chance of failure before 14.36 log seconds or 480 hours. When using six theta values this 1% percentile is estimated at 14.85 log seconds or 780 hours—Fig. 3c. Fig. 3b shows the failure time distribution at 480 MPa derived using four theta values. This distribution shows that there is only a 1% chance of failure before 15.57 log seconds or 1606 hours.

Fig. 4a shows the failure time distribution at 580 MPa derived using four theta values and the Monkman–Grant failure criteria. Of interest is the lower bound of this distribution showing that there is only a 1% chance of failure before 14.2 log seconds or 410 hours (compared to the 480 hours obtained using the rupture strain relation). When using six theta values this 1% percentile is estimated at 14.07 log seconds or 360 hours—Fig. 4c. Fig. 4b shows the failure time distribution at 480 MPa derived using four theta values. This distribution shows that there is only a 1% chance of failure before 15.41 log seconds or 1368 hours (compared to the 1606 hours obtained using the rupture strain relation).

Finally Figs 5a–d identify the important determinants of predicted times to failure using the stochastic theta model. The values for δ have been standardised so that a δ value of zero indicates that there is no significant relationship between the ln time to failure and the potential determinant associated with that δ value, whilst a δ value of 1 or -1 indicates a 1 or -1 standard deviation change in ln time to failure for a 1 standard deviation change in the potential determinant associated with that δ value. Figs 5a and b show that ε_F, $\ln(\theta_3)$ and $\ln(\theta_4)$ are the major determinants of ln time to failure when using a rupture strain as a failure criteria. Figs 5c and d show that the slope of the Monkman–Grant relation, (β), together with $\ln(\theta_3)$ and $\ln(\theta_4)$ are the major determinants of ln time to failure when using the Monkman–Grant as the failure criteria.

6. Conclusions and suggestions for future research

A number of conclusions can be drawn from the results shown above. First, there is substantial scatter in the estimates made of $\ln(\theta_j)$ at unchanging test conditions and that the distributions for each $\ln(\theta_j)$ are very different—with only some of them being normally distributed. Secondly, the major determinants of time to failure are $\ln(\theta_4)$ and rupture strain or $\ln(\theta_4)$ and the slope of the Monkman–Grant relation. As such it is essential to model the tertiary stages of creep correctly if an accurate time to failure prediction is to be made. Third, the empirical failure time distributions are not normal and generally have a long tail reaching out to higher failure times—although the failure distributions are more symmetric when using the Monkman–Grant rather than the rupture strain relation.

Finally, for Titanium 6.2.4.6 operating at 773 K and under a constant uniaxial load of 580 MPa, a service life of no more than 410 hours should be recommended. The chances of failure over this time span is then 1% or less. At a constant uniaxial load of 480 MPa and 773 K the recommended service life is 1368 hours—again with a 1% or less chance of failure over this time span. This technique can be used to obtain 1% percentile predictions at any other stress or indeed a prediction corresponding to a smaller chance of failure.

However, as the model stands, it can't predict the life of this alloy when used as turbine blades and disks. This is because during take off, flight and landing these components are subjected to varying stresses and temperatures and the loads tend to be multi rather than uniaxial. Hence possible areas of future research are to apply the stochastic model to multiaxial creep test data

and to build into the model the sum of damage accumulated over periods of varying stresses. It would also be of interest to apply the model to nonmetallic materials and to fatigue data in the ways suggested in Section 3.

Acknowledgements

The author would like to thank Rolls-Royce (supported by the D.T.I.-CARAD) for the supply of forged specimens.

References

1. R. W. EVANS, I. BEDEN and B. WILSHIRE, in 2nd International Conference on 'Creep and Fracture of Engineering Materials and Structures,' edited by B. Wilshire and D. R. J. Owen, Swansea, 1984 (Pineridge Press, Swansea, 1984) p. 1277.
2. R. W. EVANS, M. R. WILLIS, B. WILSHIRE, S. HOLDSWORTH, B. SENIOR, A. FLEMING, M. SPINDLER, and J. A. WILLIAMS, in Proceedings of the 5th International Conference on 'Creep and Fracture of Materials and Structures,' Swansea 1993, edited by B. Wilshire and R. W. Evans (The Institute of Materials, London, 1993) p. 633.
3. R. W. EVANS, *Materials Science and Technology* **16** (2000) 6.
4. P. H. MORTON, Rosenhain Centenary Conference, The Royal Society (1975).
5. A. GREASLEY, *Materials Science and Technology* **13** (1997) 31.
6. R. W. BAILEY, *in Proc. I. Mech. E.* **131** (1935).
7. F. GAROFALO, in "Fundamentals of Creep and Creep Rupture in Metals" (Macmillan, New York, 1965).
8. R. W. EVANS, *Materials Science and Technology* **5** (1989) 699.
9. R. W. EVANS and P.J. SCHARNING, *Materials Science and Technology* **17** (2001) 487.
10. M. EVANS, *Journal of Strain Analysis* **35** (5) (2000) 389.
11. *Idem*., *Journal of Materials Science* **35** (2000) 2937.
12. W. H. GREENE, in "Econometric Analysis" (Prentice Hall, New Jersey, 2000) p. 127.
13. R. L. PRENTICE, *Biometrika* **61** (1974) 539.
14. M. EVANS, *Materials Science and Technology* **12** (1996) 149.
15. J. F. LAWLESS, in "Statistical Models and Methods for Lifetime Data" (John Wiley & Sons, New York, 1982) Appendix B.
16. F. C. MONKMAN and N. J. GRANT, *Proc.* ASTM **56** (1956) 593.
17. Palisade Corporation, "@Risk: Advanced Risk Analysis for Spreadsheets" (Palisade Corporation, New York, 2000).
18. J. J. THOMAS, in "An Introduction to Statistical Analysis for Economists" (Weidenfeld and Nicolson, London, 1983) p. 190.
19. M. R. BACHE and W. J. EVANS, *International Journal of Fatigue* **14** (5) (2000) 331.
20. P. C. PARIS and F. ERDOGAN, *J. Bas Eng., ASME series D* **85** (1963) 528.
21. R. W. EVANS and B. WILSHIRE, in "Introduction to Creep" (Institute of Materials, Bournemouth, 1993) p.11.
22. M. EVANS and A.R. WARD, *Materials Science and Technology* **16** (2000) 1149.

Received 28 August 2000
and accepted 13 May 2001